JACS
JOURNAL OF THE AMERICAN CHEMICAL SOCIETY
Article
pubs.acs.org/JACS

A Theoretical Study of an Unusual Y-Shaped Three-Coordinate Pt Complex: Pt(0) σ-Disilane Complex or Pt(II) Disilyl Complex?

Nozomi Takagi and Shigeyoshi Sakaki*

Fukui Institute for Fundamental Chemistry, Kyoto University, Takano-Nishihiraki-cho 43-4, Sakyo-ku, Kyoto 606-8103, Japan

Supporting Information

ABSTRACT: The unusual Y-shaped structure of the recently reported three-coordinate Pt complex Pt[NHC(Dip)$_2$](SiMe$_2$Ph)$_2$ (NHC = N-heterocyclic carbene; Dip = 2,6-diisopropylphenyl) was considered a snapshot of the reductive elimination of disilane. A density functional theory study indicates that this structure arises from the strong trans influence of the extremely σ-donating carbene and silyl ligands. Though this complex can be understood to be a Pt(II) disilyl complex bearing a distorted geometry due to the Jahn−Teller effect, its ^{195}Pt NMR chemical shift is considerably different from those of Pt(II) complexes but close to those of typical Pt(0) complexes. Its Si···Si bonding interaction is ∼50% of the usual energy of a Si−Si single bond. The interaction between the Pt center and the (SiMe$_2$Ph)$_2$ moiety can be understood in terms of donation and back-donation interactions of the Si−Si σ-bonding and σ*-antibonding molecular orbitals with the Pt center. Thus, we conclude that this is likely a Pt(0) σ-disilane complex and thus a snapshot after a considerable amount of the charge transfer from disilane to the Pt center has occurred. Phenyl anion (Ph$^-$) and [R−Ar]$^-$ [R−Ar = 2,6-(2,6-*i*Pr$_2$C$_6$H$_3$)$_2$C$_6$H$_3$] as well as the divalent carbon(0) ligand C(NHC)$_2$ also provide similar unusual Y-shaped structures. Three-coordinate digermyl, diboryl, and silyl−boryl complexes of Pt and a disilyl complex of Pd are theoretically predicted to have similar unusual Y-shaped structures when a strongly donating ligand coordinates to the metal center. In a trigonal-bipyramidal Ir disilyl complex [Ir{NHC(Dip)$_2$}(PH$_3$)$_2$(SiMe$_3$)$_2$]$^+$, the equatorial plane has a similar unusual Y-shaped structure. These results suggest that various snapshots can be shown for the reductive eliminations of the Ge−Ge, B−B, and B−Si σ-bonds.

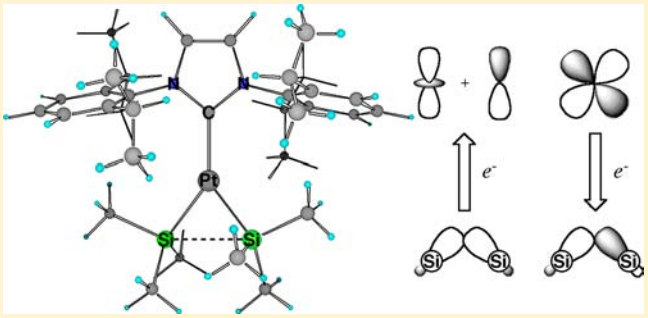

INTRODUCTION

Three-coordinate, 14-electron d^8 complexes MLR$_2$ [M = Pd(II), Pt(II); L = neutral ligand; R = hydride, alkyl, silyl, etc.) are believed to be important intermediates in various catalytic cycles for carbon−carbon and carbon−heteroatom bond formations.[1] In general, such complexes are reactive and easily undergo the fourth coordination by solvent or agostic interactions.[2] Thus, it is not easy to isolate a pure three-coordinate d^8 complex. In this regard, a bulky ligand is useful to prevent such fourth coordination sterically.[3] One of the successful examples is the synthesis of a palladium(II) aryl amido complex reported by Yamashita and Hartwig.[4] This complex does not take a sterically favorable D_{3h}-like planar structure but instead adopts a sterically unfavorable T-shaped structure. The reason for this had previously been discussed by Hoffmann and co-workers,[5] who clearly interpreted the formation of the T-shaped structure of [Au(CH$_3$)$_3$] on the basis of the Jahn−Teller effect.

From this viewpoint, the recently reported three-coordinate Pt complex Pt[NHC(Dip)$_2$](SiMe$_2$Ph)$_2$ (**1a**) (NHC = N-heterocyclic carbene; Dip = 2,6-diisopropylphenyl) bearing a bulky carbene ligand is of considerable interest,[6] as follows: (i) Its X-ray structure shows an unusual Y-shaped geometry in which the Si−Pt−Si angle is very acute and actually far from the ideal values for both the trigonal-planar and T-shaped structures. (ii) This has been understood to be a Pt(II) complex, though the theoretical analysis by Hoffmann and co-workers suggests that the Y-shaped d^8 metal complex is less stable than the T-shaped one.[5] (iii) This unusual structure is understood to be a "snapshot" of the reductive elimination of PhMe$_2$Si−SiMe$_2$Ph.[6] Thus, providing theoretical insight into the essential difference between the electronic structures of this unusual Y-shaped structure and the well-known T-shaped structure would be worthwhile. Such insight would be indispensable for a better understanding of coordinatively unsaturated complexes of d^8 metals. Also, the theoretical prediction of new complexes bearing such an unusual structure would be interesting for the further development of the chemistry of three-coordinate transition-metal complexes.

In this communication, we report a comprehensive theoretical investigation of the geometry and electronic structure of the three-coordinate Pt complex Pt[NHC(Dip)$_2$](SiMe$_2$Ph)$_2$. Our purposes here are to elucidate the nature of the bonding and the electronic structure, in particular to show which oxidation state (0 or +II) the Pt center takes, to disclose the factors necessary for the unusual Y-shaped structure, and to make theoretical

Received: May 7, 2012
Published: June 10, 2012

   dx.doi.org/10.1021/ja304110h | J. Am. Chem. Soc. 2012, 134, 11749−11759

predictions of new complexes bearing similar unusual Y-shaped structures.

MODELS AND COMPUTATIONAL DETAILS

In the present work, we investigated three kinds of geometry: **a**, **b**, and **c**, as shown in Scheme 1. Geometry **a** represents the unusual Y-shaped structure of **1a**, while **b** is a T-shaped structure with one large and one small C−Pt−Si angle and **c** is a T-shaped structure in which both C−Pt−Si angles are small (close to 90°). The model complex $Pt[NHC(Dip)_2](SiMe_3)_2$ (**2**) was reconstructed from **1a** by substituting $SiMe_3$ for $SiMe_2Ph$ (see Scheme 1). The geometry optimization of **2a** reproduced well characteristic features of the X-ray structure of **1a**, indicating that the Ph substituent of the silyl group does not significantly influence the molecular structure and that **2a** is a good model of **1a**. In this work, **2a** was employed as a realistic model for discussion. In addition to **2a**, we employed various substituents for the NHC ligand and the silyl group, as shown in Scheme 1.

Scheme 1

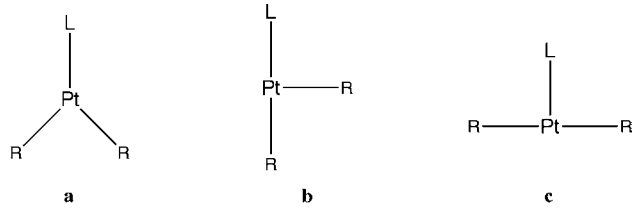

1 : L = $NHC(Dip)_2$, R = $SiMe_2Ph$
2 : L = $NHC(Dip)_2$, R = $SiMe_3$
3 : L = $NHC(Ph)_2$, R = $SiMe_3$
4 : L = NHC, R = $SiMe_3$
5 : L = NHC, R = SiH_3

All of the geometries were optimized by the DFT method with the B3PW91 functional.[7,8] For Pt, Ir, and Pd, the LANL2DZ basis set was employed,[9] with their core electrons replaced by effective core potentials (ECPs).[9] The 6-31G(d) basis set was used for the other elements.[10] This basis set system is denoted as BS-I. The optimized geometry of the real complex **1a** at the B3PW91/BS-I level agreed well with the experimentally reported X-ray structure (see Table S1 in the Supporting Information).

A better basis set system, denoted as BS-II, was employed for the evaluation of relative stability and the analysis of the electronic structure. In BS-II, the (311111/22111/411/11) basis set was employed for Pt, Ir, and Pd[11,12] with the ECPs of the Stuttgart−Dresden−Bonn group.[13] The 6-311G(d) basis set was used for the other elements. ^{195}Pt NMR chemical shifts were calculated by the DFT method with the Douglas−Kroll−Hess second-order scalar relativistic Hamiltonian[14] using the DK3-Gen-TK/NOSeC-V-TZP all-electron basis set for Pt,[15] the cc-pVTZ basis set for Si and Ge,[16] and the 6-311G(d) basis set for the other elements. This basis set system is denoted as BS-III. The M06L functional[17] was employed for the calculation of ^{195}Pt NMR chemical shift after careful comparison with the B3PW91, B3LYP,[7,18] M06,[19] LC-BLYP,[20] and HCTP[21] functionals (see Table S2 in the Supporting Information). All of the calculations were carried out with the Gaussian 03[22] and Gaussian 09[23] program packages.

RESULTS AND DISCUSSION

1. Geometrical Features of the Unusual Y-shaped Complex $Pt[NHC(Dip)_2](SiMe_3)_2$. The optimized geometry of **2a** is shown in Figure 1; see Table S1 in the Supporting Information for the geometrical parameters. It is apparent that this optimized geometry agrees well with the X-ray structure. The calculated Si−Pt−Si angle is very acute (80.3°) and is almost the same as the experimental value (80.9°). This angle is considerably different from that of typical trigonal-planar structure (120°). This acute angle and the much larger C−Pt−Si angle of 139.8° are literally consistent with the representation "unusual Y-shaped complex". The small Si−Pt−C−N dihedral angle of 27.3° shows that the Si−Pt−Si moiety is almost planar with respect to the carbene ligand $NHC(Dip)_2$. It is noted that the corresponding T-shaped **2b**, which is the usual structure for a three-coordinate Pt(II) complex, is also located at a minimum. Surprisingly, **2b** is slightly less stable than the Y-shaped **2a** by only 0.1 kcal/mol. A similar small energy difference was reported in the previous work.[6] In **2b**, the C−Pt−Si angles are 151.6° and 124.3°, which considerably deviate from those of the ideal T-shaped structure (180° and 90°, respectively). It is likely that these deviations arise from the steric repulsion between $NHC(Dip)_2$ and $SiMe_3$. The core structure becomes nonplanar to reduce the steric repulsion, as shown by the larger Si−Pt−C−N dihedral angles of 55.0° and 53.7°. Though the geometry of **2b** is considerably different from the Y-shaped structure **2a**, the Si−Pt−Si angle (84.0°) is very acute and the Si···Si distance is similar to that in **2a**.

In **3** (Scheme 1), which was constructed from **2** by replacing the terminal Dip groups with smaller phenyl (Ph) groups, only the T-shaped structure (**3b**) was optimized (see Figure S1 and Table S1 in the Supporting Information for the geometrical details). Y-shaped **3a** optimized under C_2 symmetry is not the equilibrium structure; it exhibited one small imaginary frequency (5.3i cm^{-1}), and the full geometry optimization of **3a** without constraints led to the T-shaped structure **3b**. This result implies that the *i*Pr group in Dip plays a crucial role in presenting the unusual Y-shaped structure, probably as a result of steric repulsion between the *i*Pr and $SiMe_3$ groups. In **4** (Scheme 1), which was constructed from **2** by replacing the Dip groups with H atoms, a similar result was obtained because of the much smaller steric effect (see Figure S1 and Table S1 for the geometrical details). In **5**, which was constructed from **4** by replacing the $SiMe_3$ groups with smaller SiH_3 groups, the T-shaped structure **5b** was optimized, as shown in Figure 1. Also, another T-shaped structure, **5c**, in which the two SiH_3 groups are at the positions trans to each other, was optimized as a local minimum. However, the Y-shaped structure **5a** could not be optimized; **5a** optimized under C_2 symmetry exhibited two imaginary frequencies (39.7i and 5.0i cm^{-1}).

The relative energies of three isomers are summarized in Table 1. In the smallest model, **5**, the relative stabilities were evaluated by various computational methods. Though the relative stabilities of **5a** and **5c** were sensitive to the computational method, the B3PW91-calculated energies agreed well with those of CCSD(T). Complex **5b** is the most stable, with **5a** being moderately less stable and **5c** much less stable than **5b**. Because of the small size of the NHC and silyl ligands in **5**, it is likely that the relative stabilities of **5a**, **5b**, and **5c** are mainly determined by electronic factors; in other words, the steric effect of the bulky substituent on the carbene ligand is indispensable in providing the unusual Y-shaped geometry. (See Table S3 and page S8 in the Supporting Information for relative stabilities with zero-point energy corrections and Gibbs energies.)

2. Electronic Structure of the Unusual Y-shaped Complex $Pt[NHC(Dip)_2](SiMe_3)_2$. To disclose the electronic structure of **2a**, we focus on the interaction between the Pt center and the silyl groups. The acute Si−Pt−Si angle (80.3°) and the short Si···Si distance (3.025 Å) in **2a** suggest that some bonding interaction between the two Si atoms exists. If the Si···Si bonding interaction is strong enough, **2a** would be understood as a σ-disilane complex of Pt(0), as shown in Scheme 2. If not, **2a** would be understood as a Pt(II) disilyl complex. In this understanding,

dx.doi.org/10.1021/ja304110h | J. Am. Chem. Soc. 2012, 134, 11749−11759

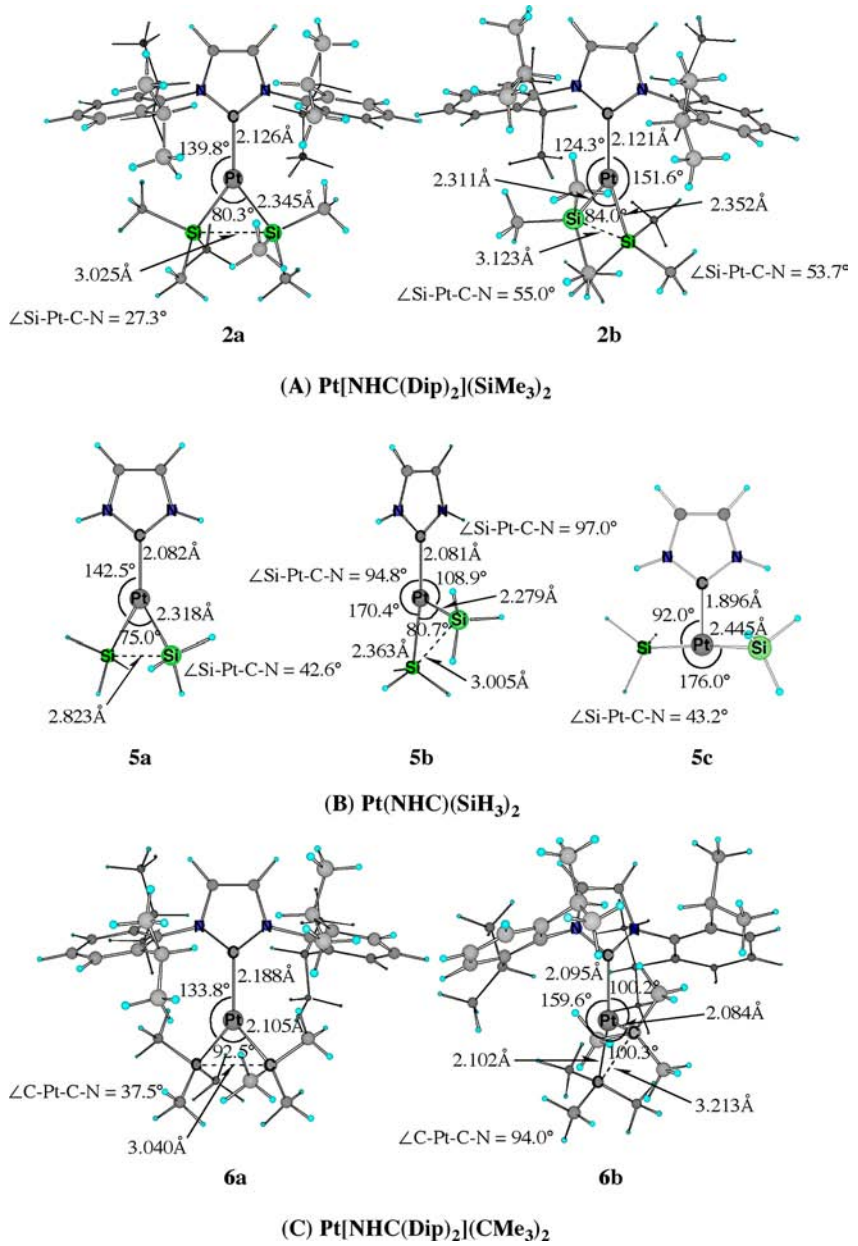

Figure 1. Optimized structures of the Pt complexes **2**, **5**, and **6** with forms **a**, **b**, and **c** at the B3PW91/BS-I level; see Scheme 1 for **a**, **b**, and **c**. Forms **2c** and **6c** could not be optimized.

the origin of the unusual Y-shaped geometry with the very acute Si−Pt−Si would be the Jahn−Teller effect.[5]

The Si···Si distance of 3.025 Å in **2a** is 28% longer than the length of the optimized Si−Si single bond (2.364 Å)[24a] of hexamethyldisilane, $Me_3Si-SiMe_3$, as shown in Table 2. The Si−Si bond energy of the distorted $Me_3Si\cdots SiMe_3$ moiety, which is taken from the optimized structure of **2a**, was calculated to be 24.9 kcal/mol at the DFT(B3PW91) level and 30.6 kcal/mol at the CCSD(T) level, representing 35% and 40% of the Si−Si bond energy of free $Me_3Si-SiMe_3$ at the DFT and CCSD(T) levels,[24b] respectively (Table 2). The Wiberg bond index between these two Si atoms was calculated to be 0.79, which is moderately smaller than that in $Me_3Si-SiMe_3$ (0.92). These results suggest that a Si−Si bonding interaction exists in **2a**. Completely different results were found for the carbon analogue **6a**, which will be discussed in the next section.

Here we discuss the interaction between Pt[NHC(Dip)$_2$] and the distorted $Me_3Si\cdots SiMe_3$ unit. As shown in Figure 2, the highest occupied molecular orbital (HOMO) and lowest unoccupied molecular orbital (LUMO) of the distorted disilane moiety are the Si−Si σ-bonding and σ^*-antibonding MOs, respectively. In **2a**, the electron population of the Si−Si σ-bonding MO is 1.393e, which is much smaller than the population of 2.0e in free disilane (see page S13 in the Supporting Information for details of this analysis). The missing population is found in the LUMO of the Pt moiety (0.671e), which consists of the $5d_{z^2}$ and 6p orbitals of the Pt center, as shown in Figure 2. On the other hand, the electron population of the Si−Si σ^*-antibonding MO increases to 0.307e, which also agrees well with the missing population in the HOMO−4 of the Pt moiety (d_{yz}). These results show that donation and back-donation interactions are strongly formed between Pt[NHC(Dip)$_2$] and the distorted $Me_3Si\cdots SiMe_3$ moiety. On the basis of the electron populations of the Si−Si σ-bonding and σ^*-antibonding MOs, the Si−Si bond order in **2a** is estimated to be 0.54, which is consistent with

dx.doi.org/10.1021/ja304110h | J. Am. Chem. Soc. 2012, 134, 11749−11759

Table 1. Relative Energies (in kcal/mol)[a] of 1−5 in Different Forms a, b, and c[b] at Various Computational Levels

complex	level	a	b	c
1	B3PW91/BS-II	0.0	+0.8	–
	MP2/BS-II	0.0	+5.2	–
	SCS-MP2/BS-II	0.0	+4.1	–
2	B3PW91/BS-II	0.0	+0.1	–
	MP2/BS-II	0.0	+1.6	–
	SCS-MP2/BS-II	0.0	+1.1	–
3	B3PW91/BS-II	0.0	−0.7	–
	MP2/BS-II	0.0	+1.3	–
	SCS-MP2/BS-II	0.0	+0.9	–
4	B3PW91/BS-II	0.0	−0.9	–
	MP2/BS-II	0.0	+1.3	–
	SCS-MP2/BS-II	0.0	+0.6	–
5	B3PW91/BS-II	0.0	−1.0	+20.3
	MP2/BS-II	0.0	+1.4	+32.6
	SCS-MP2	0.0	+0.8	+30.7
	MP3/BS-II	0.0	−1.3	+21.8
	MP4(D)/BS-II	0.0	−0.1	+26.0
	MP4(DQ)/BS-II	0.0	−0.2	+26.3
	MP4(SDQ)/BS-II	0.0	−0.3	+26.0
	MP4(SDTQ)/BS-II	0.0	+1.0	+29.1
	CCSD(T)/BS-II	0.0	−0.9	+22.8

[a]A positive or negative value indicates that the species is less or more stable, respectively, than the **a** form. The geometries were optimized at the B3PW91/BS-I level. [b]See Scheme 1.

Scheme 2

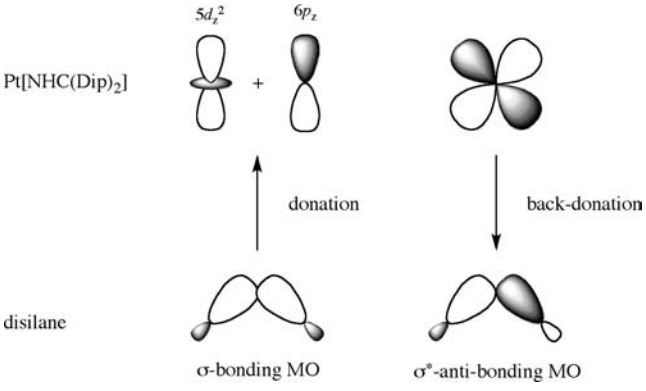

the Si−Si bond energy of the distorted disilane. All of these results are consistent with the experimental proposal that **1** can be understood as a snapshot of the reductive elimination of disilane.[6]

The Si−Si bond length, the bond energy, and the electron population analysis suggest that **2a** contains the character of Pt(0) to a considerable extent; in other words, it is likely that this complex consists of Pt(0)[NHC(Dip)$_2$] and the distorted disilane through the donation and back-donation interactions. A similar discussion of the oxidation state of Pd in the hexakis(silyl)paradium complex was presented previously.[25] Though the Si···Si bond of the distorted disilane is considerably weaker than the usual Si−Si single bond, the interaction between the Pt center and the distorted Si−Si bond stabilizes the distorted disilane moiety, suggesting that the Si−Si bond is stronger in **2a** than in the distorted free disilane.

At the end of this section, we wish to mention the electronic structures of **4c** and **5c**, which contain separately coordinated silyl groups. The silyl group is usually considered to be an anion in a formal sense when it is bound to a metal center. Because no interaction exists between the two silyl groups in **4c** and **5c**, the oxidation state of the Pt center is understood to be +II. Consistent with this understanding, the Pt d orbital population is somewhat smaller in **4c** and **5c** than in **4a**, **4b**, **5a**, and **5b**.

3. Comparison of Pt[NHC(Dip)$_2$](SiMe$_3$)$_2$ with Carbon Analogues. A comparison between the silicon complex **2** and the carbon analogue Pt[NHC(Dip)$_2$](CMe$_3$)$_2$ (**6**) provides a good understanding of the geometry and electronic structure of **2**. Complex **6** takes a typical T-shaped geometry (**6b**), as shown in Figure 1. In **6b**, the C−C distance is very long, indicating that two CMe$_3$ ligands separately coordinate to the Pt center. Thus, **6b** is classified as a typical Pt(II) complex. The Y-shaped structure **6a** was optimized under constraint of C_2 symmetry but exhibited one imaginary frequency (79.0i cm^{-1}). This Y-shaped structure is completely different from that of **2a**, as follows: (i) the C···C distance of 3.040 Å is very long, about 2 times longer than that of free Me$_3$C−CMe$_3$ (1.582 Å)[24a] (Table 2), and (ii)

Table 2. Bond Length, Wiberg Bond Index (WBI), Bond Energy (BE), HOMO and LUMO Energies, and Bond Order of the Me$_3$E−EMe$_3$ Moiety (E = C, Si, Ge) in Free Me$_3$E−EMe$_3$ ("Equilibrium Structure") and in the Pt[NHC(Dip)$_2$](EMe$_3$)$_2$ Complex ("Distorted Structure") Calculated at the B3PW91/BS-II//B3PW91/BS-I Level

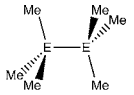
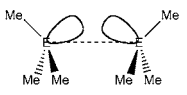

	equilibrium structure	*distorted structure*
	E = C	
C-C (Å)	1.582	3.040
WBI_{C-C}	0.94	0.64
BE (kcal/mol)	66.9 (83.2)[a]	-37.2 (-13.7)[a]
LUMO (eV)	+1.16	-2.64
HOMO (eV)	-8.20	-5.01
Bond Order	1.0	0.41
	E = Si	
Si-Si (Å)	2.364	3.025
WBI_{Si-Si}	0.92	0.79
BE (kcal/mol)	71.2 (76.2)[a]	24.9 (30.6)[a]
LUMO (eV)	+0.89	-1.52
HOMO (eV)	-6.75	-5.79
Bond Order	1.0	0.54
	E = Ge	
Ge-Ge (Å)	2.439	3.031
WBI_{Ge-Ge}	0.90	0.77
BE (kcal/mol)	66.2 (71.1)[a]	26.6 (32.1)[a]
LUMO (eV)	+0.88	-1.73
HOMO (eV)	-6.66	-5.77
Bond Order	1.0	0.63

[a]The CCSD(T)/BS-II//B3PW91/BS-I calculated value is given in parentheses.

the distorted Me$_3$C···CMe$_3$ moiety taken from the optimized structure of **6a** was calculated to be considerably less stable than the sum of two ·CMe$_3$ radicals by 37.2 kcal/mol at the DFT(B3PW91) level and 13.7 kcal/mol at the CCSD(T) level; in

dx.doi.org/10.1021/ja304110h | J. Am. Chem. Soc. 2012, 134, 11749−11759

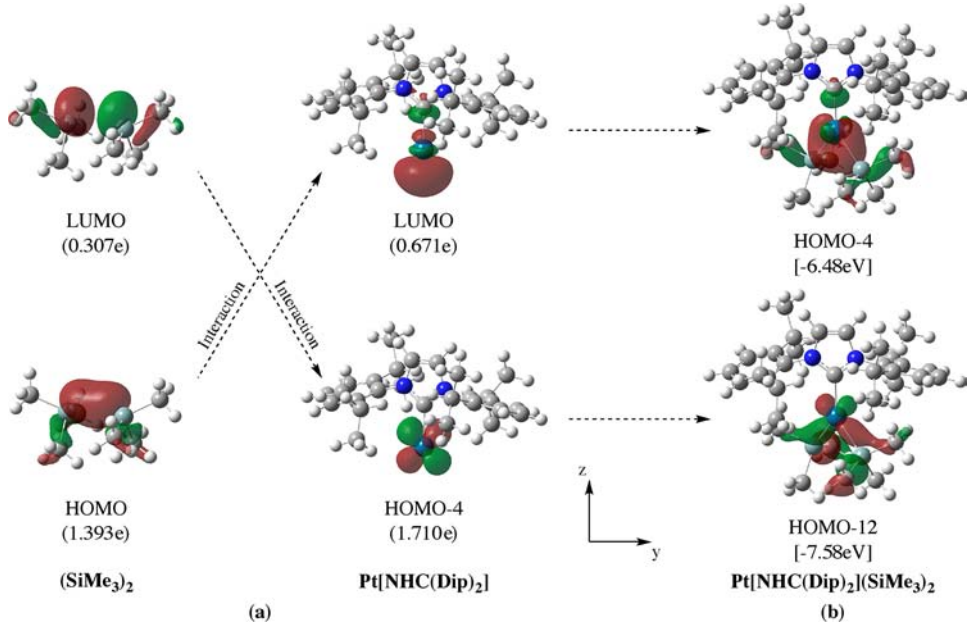

Figure 2. Kohn–Sham MOs of (a) the distorted $Me_3Si–SiMe_3$ and $Pt[NHC(Dip)_2]$ moieties and (b) **2a** at the B3PW91/BS-II/B3PW91/BS-I level. The geometries of the $Me_3Si–SiMe_3$ and $Pt[NHC(Dip)_2]$ moieties were taken to be the same as those in **2a**. The electron populations of the MOs are given in parentheses, and the MO energies are given in square brackets.

Table 3. Electron Populations[a] and ^{195}Pt NMR Chemical Shifts[b,c] for Various Pt Complexes

	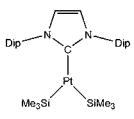 **2a**	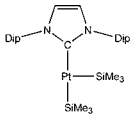 **2b**	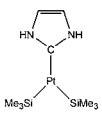 **4a**	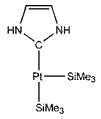 **4b**	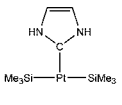 **4c**	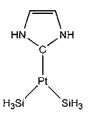 **5a**	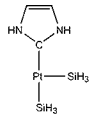 **5b**	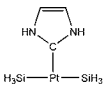 **5c**
Pt								
s	2.96	2.95	3.01	2.98	2.86	3.02	2.96	2.87
p	6.36	6.40	6.34	6.42	6.66	6.26	6.34	6.53
d	9.09	9.04	9.19	9.18	8.94	9.15	9.15	8.91
SiR_3	81.70(-0.30)[d]	81.70(-0.30)[d]	81.69(-0.31)[d]	81.70(-0.30)[d]	81.93(-0.07)[d]	33.85(-0.15)[d]	33.86(-0.14)[d]	34.19(+0.19)[d]
L	211.98(-0.02)[d]	211.91(-0.09)[d]	35.75(-0.25)[d]	35.70(-0.30)[d]	35.60(-0.40)[d]	35.69(-0.31)[d]	35.67(-0.33)[d]	35.50(-0.50)[d]
^{195}Pt NMR	-5935.8	-5856.9	-5807.2	-5381.5	-366.0	-6123.6	-5438.9	-583.4
^{195}Pt NMR (expl.)	-5493[6]	-	-	-	-	-	-	-
oxidation state	?	?	?	?	Pt(II)	?	?	Pt(II)
	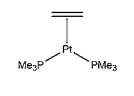 **$Pt(PMe_3)_2(C_2H_2)$**	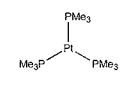 **$Pt(PMe_3)_3$**	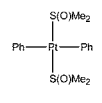 **$Pt(Ph)_2(DMSO)_2PtCl_2(NH_3)(C_2H_2)$**	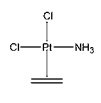	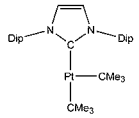 **6b**	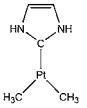 **7a**	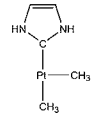 **7b**	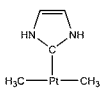 **7c**
Pt								
s	2.62	2.53	2.87	2.68	2.86	2.98	2.88	2.76
p	6.44	6.54	6.50	6.46	6.26	6.17	6.20	6.21
d	8.95	9.01	8.84	8.57	8.63	8.88	8.84	8.69
CR_3	-	-	-	-	66.32(+0.32)[d]	18.24(+0.24)[d]	18.35(+0.35)[d]	18.79(+0.79)[d]
L	-	-	-	-	211.90(-0.10)[d]	35.71(-0.29)[d]	35.69(-0.31)[d]	35.52(-0.48)[d]
^{195}Pt NMR calc.	-4851.6	-4233.3	-3884.8	-2882.8	-3497.8	-4109.0	-2942.3	-1705.0
expl.	-4658[e]	-4526[f]	-4217[g]	≈ -2700[h]	-	-	-	-
oxidation state	Pt(0)	Pt(0)	Pt(II)	Pt(II)	Pt(II)	Pt(II)	Pt(II)	Pt(II)

[a]The B3PW91/BS-II//B3PW91/BS-I method was employed. [b]The M06L/BS-III//B3PW91/BS-I method with the Douglas–Kroll–Hess second-order scalar relativistic Hamiltonian was employed. [c]$[PtCl_6]^{2-}\cdot 20H_2O$ was taken as the reference for the ^{195}Pt NMR chemical shifts, where the Pt···O distances were taken from the previous report and the further solvation effect of water was incorporated using the PCM method; see page S9 in the Supporting Information for details. [d]The value in parentheses is the population change. [e]Reported for $Pt(PPh_3)_2(C_2H_2)$; see ref 31. [f]Reported for $Pt(PEt_3)_3$; see ref 32. [g]Reported for $Pt(Ph)_2(DMSO)_2$; see ref 33. [h]Reported for $PtCl_2[NH_2(CHMePh)][CH_2CH(CHMeOH)]$; see ref 34.

other words, no bonding interaction exists between two CMe_3 groups. These results clearly indicate that **6a** should be understood to be a Pt(II) complex consisting of $[Pt(II)\{NHC(Dip)_2\}]^{2+}$ and two CMe_3 ligands. In a smaller model complex of the carbon analogue $Pt(NHC)(CH_3)_2$ (**7**), **7b** is the most stable, while **7a** and **7c** are less stable than **7b** by 10.1 and 10.0 kcal/mol, respectively. It should be noted that like the silicon complex **5** but unlike the bulky carbon analogue **6**, **7c** was located as a

dx.doi.org/10.1021/ja304110h | J. Am. Chem. Soc. 2012, 134, 11749–11759

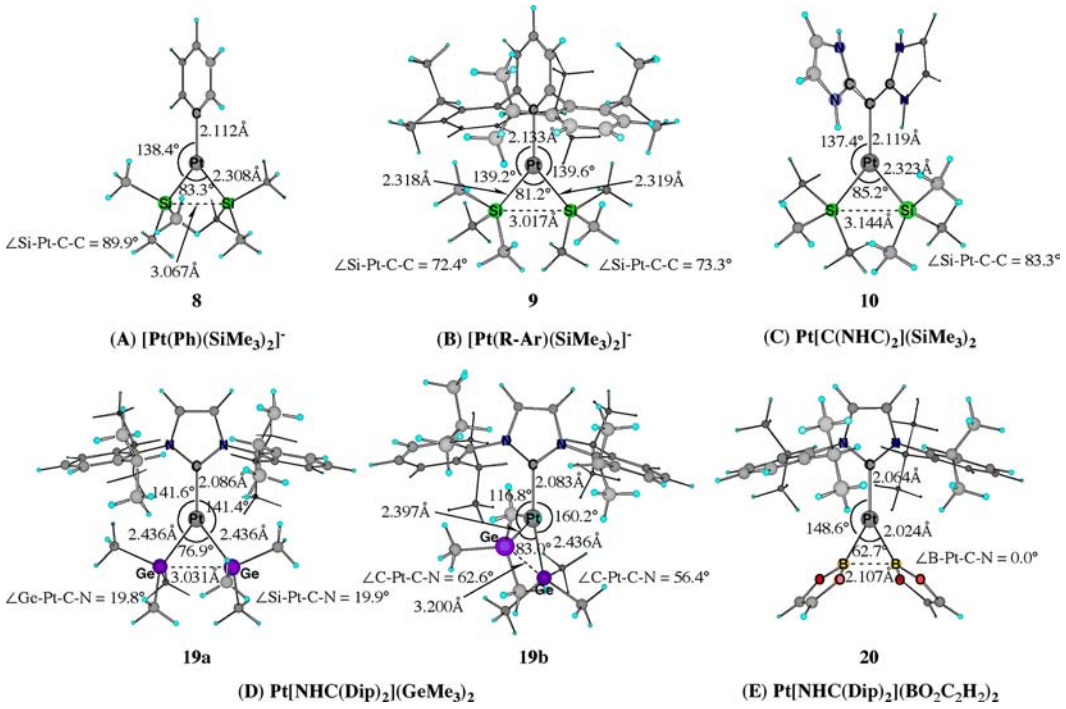

Figure 3. Structures of the Y-shaped Pt complexes **8**, **9**, **10**, **19**, and **20** optimized at the B3PW91/BS-I level.

minimum, indicating that the large steric factor gives rise to destabilization of **6c**.

The d-electron populations are similar to each other in **6b**, **7a**, **7b**, and **7c** but considerably smaller than those of the silicon analogues **2**, **4**, and **5**, as shown in Table 3. Also, one d orbital was found in the unoccupied level in **6b**, **7a**, **7b**, and **7c** but could not be found in **2**, **4**, and **5** (Figure S2 in the Supporting Information). This is one piece of evidence that **6b**, **7a**, **7b**, and **7c** should be understood to be Pt(II) complexes.

4. ^{195}Pt NMR Chemical Shift and Pt Oxidation State. It is of considerable interest to evaluate the ^{195}Pt NMR chemical shifts of these complexes, because the ^{195}Pt NMR chemical shift is one of the indexes for the electronic structure of the Pt center; for instance, ^{195}Pt NMR chemical shifts of Pt(IV) complexes are found in the range −6000 to 200 ppm, those of Pt(II) complexes in the range −4200 to −2700 ppm, and those of Pt(0) complexes around −4600 ppm.[26,27] Here we evaluated the ^{195}Pt NMR chemical shift at the DFT(M06L)/BS-III level, taking $[PtCl_6]^{2-}\cdot 20H_2O$ as a reference, with the 20 H_2O molecules included in the reference system because solvation by water molecules significantly influences the ^{195}Pt NMR chemical shift[28,29] (see Table S2 and page S9 in the Supporting Information for details). Further solvation effects were incorporated with the polarized continuum model (PCM).[30] The M06L-calculated ^{195}Pt NMR chemical shift becomes less negative in the order **2a** > $Pt(PMe_3)_2(C_2H_4)$[31] > $Pt(PMe_3)_3$[32] > $Pt(Ph)_2(DMSO)_2$[33] > *cis*-$PtCl_2(NH_3)(C_2H_4)$,[34] as shown in Table 3. This trend agrees with the experimental one, indicating that we can use the M06L-calculated ^{195}Pt NMR chemical shift for discussion. It is noted that the experimental and calculated ^{195}Pt NMR chemical shifts for **2a** are more negative than those of the typical Pt(0) complexes $Pt(PMe_3)_2(C_2H_4)$ and $Pt(PMe_3)_3$, as shown in Table 3. The ^{195}Pt NMR chemical shifts calculated for the Y-shaped **4a** and **5a** and the T-shaped **2b**, **4b**, and **5b** are similar to that for **2a**, indicating that the electronic structures of the Pt centers of these complexes are similar to that of **2a**. On the other hand, the ^{195}Pt NMR chemical shift of **5c** is substantially different from those of **2a**, **2b**, **4a**, **4b**, **5a**, and **5b**. Because the Pt oxidation state of **5c** is understood to be +II, as discussed above, these ^{195}Pt NMR chemical shifts indicate that the Pt oxidation state of **2a** is different from +II.

The ^{195}Pt NMR chemical shifts of typical Pt(II) complexes are observed in the range −2700 to −4200 ppm (Table 3). The experimental ^{195}Pt NMR chemical shift for $Pt(Ph)_2(DMSO)_2$ is not very much different from that of $Pt(PMe_3)_3$ but is still less negative than those of all the Pt(0) complexes. Thus, it is concluded that the ^{195}Pt NMR chemical shift of the Pt(II) complex is less negative than that of the Pt(0) complex. In Pt(NHC)-$(CH_3)_2$ (**7**), which is the carbon analogue of **5**, the ^{195}Pt NMR chemical shift was calculated to be −2942 and −1705 ppm for the T-shaped complexes **7b** and **7c**, respectively, and −4109 ppm for Y-shaped **7a**. Though the chemical shift of **7a** is considerably negative, it is still in the range for Pt(II) complexes. These results are consistent with our understanding that the carbon analogues **7a**, **7b**, and **7c** are Pt(II) complexes, as discussed in the former section.

In conclusion, the ^{195}Pt NMR chemical shifts of **2a**, **2b**, **4a**, **4b**, **5a**, and **5b** are considerably different from those of typical Pt(II) complexes but similar to those of typical Pt(0) complexes. These results suggest that **2a** should be understood as a σ-disilane complex of Pt(0) rather than a disilyl complex of Pt(II). On the basis of these suggestions, we propose that **1** is a snapshot of the reductive elimination of disilane after a considerable amount of the charge transfer from disilane to the Pt center has occurred

5. Ligand Effects on the Geometry of $PtL(SiMe_3)_2$. One of the important questions here is what ligands can be utilized to produce novel Y-shaped platinum complexes $PtL(SiMe_3)_2$. The answer to this question is indispensable for finding new three-coordinate $PtL(SiMe_3)_2$ complexes with the unusual Y-shaped structure. Also, it is of considerable interest to elucidate whether $NHC(Dip)_2$ is the only ligand that can be utilized to produce the unusual Y-shaped three-coordinate structure. Thus, phenyl anion (Ph^-), the substituted phenyl anion $[R-Ar]^-$ [R−Ar = 2,6-(2,6-*i*$Pr_2C_6H_3)_2C_6H_3$], and

dx.doi.org/10.1021/ja304110h | J. Am. Chem. Soc. 2012, 134, 11749−11759

a divalent carbon(0) compound, $C(NHC)_2$, were employed here as donor ligands. The R−Ar group has been widely used as a substituent and a ligand in the syntheses of a lot of unique compounds having an unusual bond between heavier main-group elements, between transition-metal elements, or between heavier main-group and transition-metal elements because of its characteristic and bulky structural features.[35] $C(NHC)_2$ has been recently reported as a divalent carbon(0) compound that can act as a strong donor because of the presence of two lone-pair orbitals on the central carbon atom.[36]

We found that $[Pt(Ph)(SiMe_3)_2]^-$ (**8**), $[Pt(R{-}Ar)(SiMe_3)_2]^-$ (**9**), and $Pt[C(NHC)_2](SiMe_3)_2$ (**10**) take the Y-shaped structure, as shown in Figure 3. It should be noted that the Y-shaped structure with an acute Si−Pt−Si angle was found in **8** and **10** despite the absence of steric effects such as those in **2a**, as Ph^- and $C(NHC)_2$ are much less bulky than $NHC(Dip)_2$. The Si−Pt−Si angle decreases in the order **10** > **8** > **9**. The smaller angle in **9** than in **8** arises from the larger steric effect of R−Ar. Their geometrical features are similar to those for **2a**, suggesting that these complexes have similar electronic structures. Interestingly, the T-shaped structure could not be located for any of them. On the other hand, $PtL(SiMe_3)_2$ with either a phosphine ligand [L = PMe_3 (**11**), PPh_3 (**12**), PCy_3 (**13**)] or a typical organic ligand [L = CH_3NC (**14**), CH_3CN (**15**), NMe_3 (**16**), C_5H_5N (**17**), CO (**18**)] provided only the T-shaped structure (Figure S3 in the Supporting Information).

As mentioned previously[6] and here, a strongly donating ligand is necessary for the unusual Y-shaped structure. Considering this, we reach one reasonable explanation for the unusual Y-shaped structure: The silyl ligand very strongly destabilizes the T-shaped structure **c**, because two strong silyl groups take the positions trans to each other in form **c**. Another strong NHC donor ligand destabilizes the T-shaped structure **b**, because the NHC is at the position trans to silyl in form **b**. Hence, only the Y-shaped structure **a** becomes stable.

In this regard, the trans influence is considered a good index for the Y-shaped structure. To investigate the trans influence, we employed here a model complex $PtL(SiH_3)Cl$ with an ideal T-shaped structure in which the chloride ligand is placed at the position trans to the L ligand with L−Pt−Si and Cl−Pt−Si angles of 90.0° (Scheme 3). As shown in Table 4,

Scheme 3

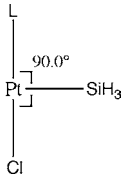

the Pt−Cl distance increases in the order CH_3CN < CO < C_5H_5N < NMe_3 < CH_3NC < PMe_3 ≈ PPh_3 < NHC < $NHC(Ph)_2$ < PCy_3 < $NHC(Dip)_2$ < $C(NHC)_2$ < $[R{-}Ar]^-$ < Ph^-. A clear correlation between the Pt−Cl distance and the stable structure is observed. The ligands that provide a long Pt−Cl distance afford the unusual Y-shaped structure. For instance, Ph^-, $[R{-}Ar]^-$, $C(NHC)_2$, and $NHC(Dip)_2$ provide a long Pt−Cl distance in $PtL(SiH_3)Cl$ and the unusual Y-shaped structure in $PtL(SiMe_3)_2$. $NHC(Dip)_2$, which provides both the Y-shaped and T-shaped structures, exhibits a smaller trans influence than $C(NHC)_2$ but a larger trans influence than PCy_3, as shown in Table 4. When the trans influence is weaker than that of $NHC(Dip)_2$, only the T-shaped structure is presented.

The next important task was to find a good measure of the trans influence. The HOMO energy is one of the determining factors for the donation strength and the trans influence. However, anions exhibit abnormally high orbital energies as a result of their negative charge. Instead of the HOMO energy, here we evaluated the proton affinity (PA) of the ligand to examine whether it is a good index of the donation strength, as shown in Table 4. Obviously, Ph^-, $[R{-}Ar]^-$, and $C(NHC)_2$ exhibit much larger PAs than the other ligands. As shown in Figure 4, a good correlation between the PA and the Pt−Cl distance was observed, except for acetonitrile (CH_3CN), trimethylamine (NMe_3) and pyridine (C_5H_5N). They present much larger PAs than expected from their Pt−Cl bond distances. It is likely that the large electronegativity of nitrogen provides a larger PA through stronger electrostatic interactions. Thus, the PA is considered here to be a good index to predict whether or not the Y-shaped structure is possible, except for nitrogen-coordinating ligands.

6. Prediction of Y-shaped Digermyl and Diboryl Complexes. Another important question is whether only the silyl group affords this unusual Y-shaped structure. We examined here germyl and boryl groups. The digermyl complex $Pt[NHC(Dip)_2](GeMe_3)_2$ (**19**) provides both Y- (**19a**) and T-shaped (**19b**) structures like **1** and **2**, as shown in Figure 3. The Y-shaped structure **19a** is only 0.6 kcal/mol more stable than **19b**. Interestingly, the Ge−Pt−Ge angle in **19a** (76.9°) is much smaller than the Si−Pt−Si angle in **2a**. As shown in Table 2, the Ge···Ge distance in **19a** (3.031 Å) is 24.3% longer than that in hexamethyldigermane Me_3Ge-$GeMe_3$ (2.439 Å).[24a] The Ge−Ge bond energy in the distorted $Me_3Ge{\cdots}GeMe_3$ moiety taken from the optimized structure of **19a** was calculated to be 26.6 kcal/mol at the DFT(B3PW91) level and 32.1 kcal/mol at the CCSD(T) level, which are 40% and 45% of the DFT(B3PW91)- and CCSD(T)-calculated bond energies of free $Me_3Ge{-}GeMe_3$ (66.2 and 71.1 kcal/mol, respectively).[24b] These results show that the Ge···Ge bonding interaction is quite strong in **19a**, much stronger than that in the silicon analogue **2a**. Population analysis of the MOs showed that the electron population of the Ge−Ge σ-bonding MO of the digermane moiety decreases to 1.567e in **19a**, which is somewhat larger than that in **2a**. The electron population of the Ge−Ge σ^*-antibonding MO increases to 0.304e, which is almost the same as that of **2a**, as shown in Figure 5a. The calculated Ge−Ge bond order of 0.63 is larger than that for the silicon analogue **2a**, which is consistent with the stronger Ge−Ge bonding interaction in **19a**.

The diboryl complex $Pt[NHC(Dip)_2](BO_2C_2H_2)_2$ (**20**) presents only the Y-shaped structure, as shown in Figure 3. The B−Pt−B angle is very acute (62.7°), and the B···B distance (2.107 Å) is 25.3% longer than that of the free diborane $[B(O_2C_2H_2)]_2$ (1.682 Å).[24a] The B−B bond energy of the distorted $H_2C_2O_2B{\cdots}BO_2C_2H_2$ moiety taken from the optimized structure of **20** was calculated to be 64.2 kcal/mol at the DFT(B3PW91) level and 67.8 kcal/mol at the CCSD(T) level, which are 57% and 59% of the DFT(B3PW91)- and CCSD(T)-calculated B−B bond energies of $[B(O_2C_2H_2)]_2$ (111.9 and 114.4 kcal/mol, respectively).[24b] This bond energy is more than half of the B−B single-bond energy. In other words, the B−B bonding interaction in the diboryl complex is much stronger than the Si−Si and Ge−Ge interactions in the disilyl and digermyl analogues. The considerably strong B−B bonding interaction as well as the small B−Pt−B angle arises from the presence of the empty p orbital on

dx.doi.org/10.1021/ja304110h | J. Am. Chem. Soc. 2012, 134, 11749−11759

Table 4. Coordinate Bond Distances in $PtL(SiH_3)Cl$,[a] HOMO Energies and Proton Affinities (PA) of Ligands L, and Equilibrium Structures of $PtL(SiMe_3)_2$ at the B3PW91/BS-II//B3PW91/BS-I Level

	Ph^-	$[R-Ar]^-$	$C(NHC)_2$	$NHC(Dip)_2$	PCy_3	$NHC(Ph)_2$	NHC	PPh_3	PMe_3	CH_3NC	NMe_3	C_5H_5N	CO	CH_3CN
Bond Distances in $PtL(SiH_3)Cl$ (Å)														
Pt−L	1.997	2.004	2.023	1.963	2.280	1.964	1.956	2.250	2.246	1.883	2.138	2.044	1.849	1.950
Pt−Cl	2.426	2.412	2.361	2.341	2.338	2.336	2.332	2.328	2.327	2.307	2.291	2.289	2.287	2.280
Pt−Si	2.265	2.260	2.275	2.288	2.300	2.298	2.298	2.309	2.300	2.321	2.291	2.296	2.351	2.307
HOMO Energies (eV) and Proton Affinities (kcal/mol) of L														
E_{HOMO}	+1.06	−0.54	−3.68	−5.98	−5.63	−6.14	−5.85	−6.01	−6.20	−8.36	−5.85	−7.11	−10.39	−9.16
PA	416.8	399.6	303.3	279.2	252.9	272.0	262.4	239.7	232.5	206.4	235.1	231.6	147.1	193.4
Structure(s) of $PtL(SiMe_3)_2$														
	Y	Y	Y	Y and T	T	T	T	T	T	T	T	T	T	T

[a]See Scheme 3.

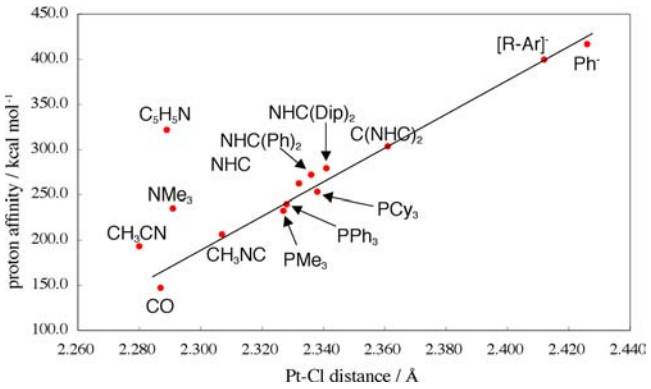

Figure 4. Proton affinity (PA) of L (kcal/mol) vs Pt−Cl distance (Å) in $PtL(SiH_3)Cl$ (see Scheme 3) at the B3PW91/BS-II//B3PW91/BS-I level.

the B atom, as follows: There are two bonding MOs between the two B atoms. One is the B−B σ-bonding MO HOMO−2 (Figure 5b), which is similar to the Si−Si σ-bonding MO. This HOMO−2 forms bonding overlap with the LUMO of the Pt moiety. Another is a bonding MO between the p_π orbitals of the B atoms (LUMO+1), which forms a bonding overlap with the doubly occupied d_σ orbital of Pt (HOMO and HOMO−2). This MO does not exist in the disilyl analogue (Figure 2a). These two kinds of bonding MOs are responsible for the stronger B−B bond and much smaller B−Pt−B angle.

Population analysis of **20** provides clear evidence for the above discussion. The electron population of the HOMO−4 (d_{yz}) of the Pt moiety decreases to 1.582e, and the population of the LUMO of the distorted diborane increases to 0.333e, as shown in Figure 5b. These population changes are larger than those in **2a**. The electron population of the B−B σ-bonding MO decreases to 1.656e, and the population of the LUMO of the Pt moiety increases to 0.382e (Figure 5b). Interestingly, the missing population in the d_σ orbitals of the Pt moiety is found in the σ-type LUMO+1 of the diborane moiety (0.118e) (see Figure 5b). The B−B σ- and π-bond orders are estimated to be 0.66 and 0.06,

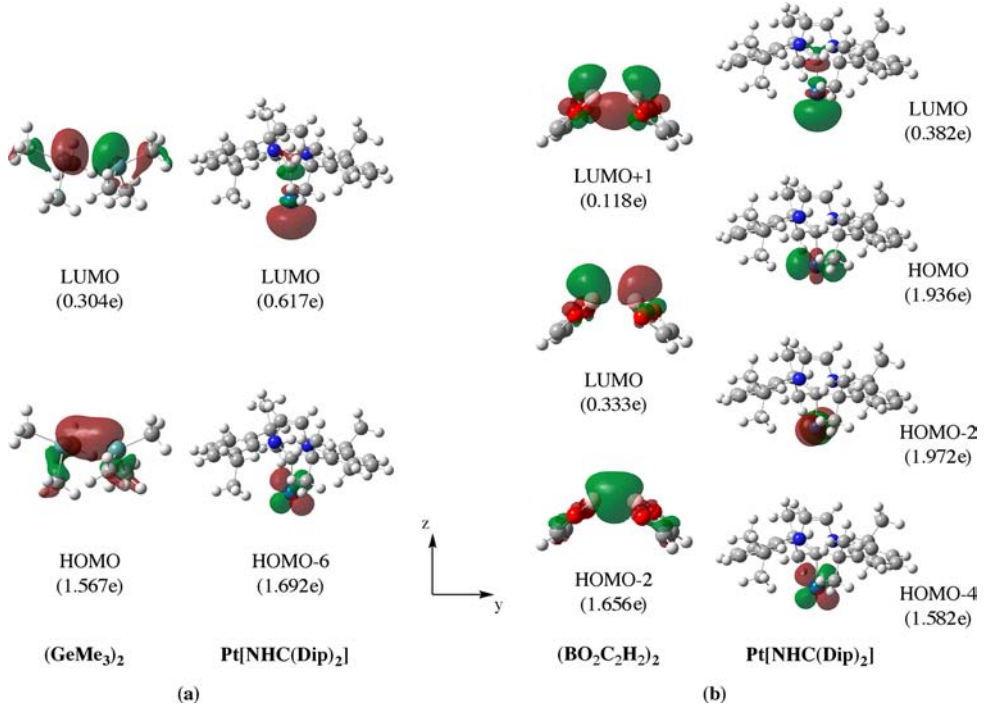

Figure 5. Kohn−Sham orbitals of the distorted $Me_3Ge-GeMe_3$ and $Pt[NHC(Dip)_2]$ moieties in **19a** and the distorted $H_2C_2O_2B-BO_2C_2H_2$ and $Pt[NHC(Dip)_2]$ moieties in **20** at the B3PW91/BS-II//B3PW91/BS-I level. The geometries of the various moieties were taken to be the same as those in the corresponding complexes. The electron populations of the MOs are given in parentheses.

dx.doi.org/10.1021/ja304110h | J. Am. Chem. Soc. 2012, 134, 11749−11759

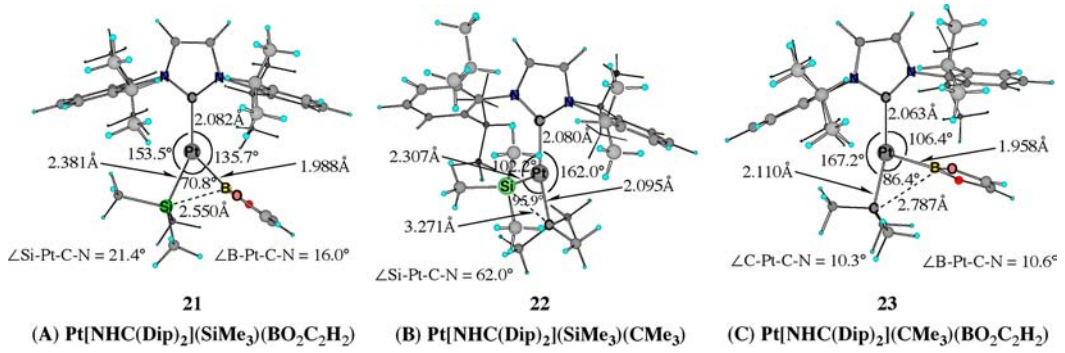

Figure 6. Structures of the Pt complexes **21**, **22**, and **23** optimized at the B3PW91/BS-I level.

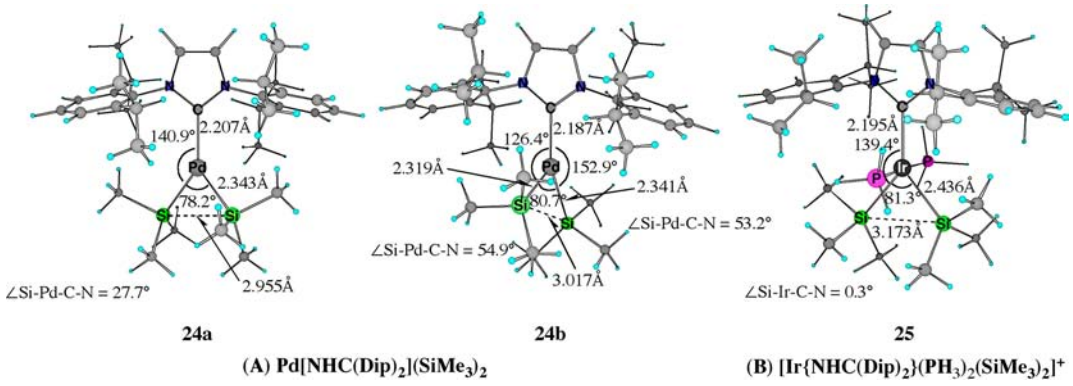

Figure 7. Structures of the Pd and Ir complexes **24** and **25** optimized at the B3PW91/BS-I level.

respectively, indicating that the σ bond in **20** is stronger than those in **2a** and **19a** and additionally that the π-bonding interaction somewhat participates in the B−B bond in **20**. As a result, **20** possesses a stronger B−B bond and more acute B−Pt−B angle in comparison with the Si−Si bond and Si−Pt−Si angle in **2a**.

The calculated ^{195}Pt NMR chemical shifts for **8**, **9**, **10**, **19a**, and **20** are −5580.5, −5525.5, −5587.3, −5690.2, and −5343.1 ppm, respectively. These chemical shifts are in the range −5300 to −5700 ppm, moderately less negative than that of **2a** (−5935.8 ppm) but still much more negative than those of typical Pt(II) complexes. Thus, the electronic structures of these complexes are similar to that of **2a**. In conclusion, both **19a** and **20** are understood to be σ-digermane and σ-diborane complexes with Pt(0)[NHC(Dip)$_2$].

Because the diborane complex exhibits geometrical features similar to those of the disilane complex, it was interesting to investigate a combination of silyl and boryl ligands in one complex, Pt[NHC(Dip)$_2$](SiMe$_3$)(BO$_2$C$_2$H$_2$) (**21**). This complex takes the deformed Y-shaped structure, as shown in Figure 6. The SiMe$_3$ group is slightly closer to the position trans to NHC(Dip)$_2$. The Si−Pt−B angle is very acute (70.8°), suggesting that a considerably strong bonding interaction is formed between the Si and B atoms. The bonding interaction is formed through similar donation from the Si−B σ-bonding MO to the Pt empty d orbital and back-donation from the doubly occupied Pt d orbital to both the Si−B σ^*-antibonding MO and the vacant p orbital of the B atom. The T-shaped structure could not be located.

We propose that **19a**, **20**, and **21** should be considered as snapshots of reductive eliminations from a digermane, diborane, and borylsilane that are similar to but shifted more toward the product side than **1** and **2a**.

If one of them is substituted with CMe$_3$, the geometry changes to the T-shaped structure, as shown for Pt[NHC(Dip)$_2$](SiMe$_3$)(CMe$_3$) (**22**) and Pt[NHC(Dip)$_2$](BO$_2$C$_2$H$_2$)(CMe$_3$) (**23**) in Figure 6. In **22** and **23**, the CMe$_3$ ligand always takes the position trans to NHC(Dip)$_2$ because the alkyl ligand is a weaker donor than the silyl and boryl ligands.[37] These geometrical features agree with the discussion that the three ligands must have a strong trans influence to achieve the unusual Y-shaped structure.

7. Prediction of Pd and Ir Complexes Bearing an Acute Si−M−Si Angle. Another interesting question was whether Pd can form the unusual Y-shaped geometry. For the Pd analogue Pd[NHC(Dip)$_2$](SiMe$_3$)$_2$ (**24**), the Y-shaped structure was located as a minimum (**24a**), as shown in Figure 7. It should be noted that the Si−Pd−Si angle (78.2°) is more acute and the Si···Si distance (2.955 Å) is shorter than the analogous features in **2a**. The donation from the disilane moiety to the Pd moiety is somewhat weaker in **24a** than that to the Pt moiety in **2a**, as indicated by the considerably smaller electron population of the LUMO of the Pd[NHC(Dip)$_2$] moiety (0.334e) in **24a** than in the analogous MO in **2a** (0.671e). The population change due to back-donation is little different between **2a** and **24a** (0.282e for **24a** and 0.307e for **2a**). As a result, the Si−Si bond order in **24a** (0.67) is somewhat larger than that in **2a** (0.54). The similar T-shaped structure **24b** was also located and found to possess an acute Si−Pd−Si angle (80.7°) and a short Si···Si distance (3.017 Å). Complex **24a** is as stable as **24b**, as shown by the calculated energy difference of 0.01 kcal/mol.

The five-coordinate Ir complex [Ir{NHC(Dip)$_2$}(PH$_3$)$_2$(SiMe$_3$)$_2$]$^+$ (**25**) was investigated, as shown in Figure 7. The geometry of the equatorial Ir{NHC(Dip)$_2$}(SiMe$_3$)$_2$ moiety resembles well that of the unusual Y-shaped Pt complex; for instance, the Si−Ir−Si angle is 81.3° and the Si···Si distance is

dx.doi.org/10.1021/ja304110h | J. Am. Chem. Soc. 2012, 134, 11749−11759

3.173 Å, similar the analogous features in **2a**. These geometrical features indicate that the considerably large bonding interaction is formed between two Si atoms in **25**. Here, the charge transfers of 1.276e from the disilane moiety to the $[Ir\{NHC(Dip)_2\}(PH_3)_2]^+$ moiety and 0.327e from the $[Ir\{NHC(Dip)_2\}(PH_3)_2]^+$ moiety to the disilane moiety occur to extents similar to those in **2a**. The T-shaped structure of this moiety could not be located, unlike **2b**.

These results for the Pd and Ir analogues of **2** lead to the prediction that this type of unusual Y-shaped geometry is not limited to Pt but is also possible for Pd and Ir.

CONCLUSIONS

The unusual Y-shaped three-coordinate Pt complex $Pt[NHC(Dip)_2](SiMe_2Ph)_2$ (NHC = N-heterocyclic carbene, Dip = 2,6-diisopropylphenyl) and its realistic model $Pt[NHC(Dip)_2](SiMe_3)_2$ were theoretically investigated. The Y-shaped structure becomes stable when three ligands are strongly donating. The upfield-shifted ^{195}Pt NMR chemical shift of the Y-shaped $Pt[NHC(Dip)_2](SiMe_2Ph)_2$ is much different from those of the Pt(II) complexes, while the ^{195}Pt NMR chemical shift of the T-shaped form **c** is similar to those of the Pt(II) complexes. A considerably strong bonding interaction is formed between the two Si atoms. On the basis of these results, we present the reasonable understanding that the unusual Y-shaped complex consists of $Pt(0)[NHC(Dip)_2]$ and a distorted disilane moiety, with the disilane coordinating to the Pt(0) center through donation and back-donation interactions. The donation occurs from the Si−Si σ-bonding MO to the Pt moiety, and the back-donation is from the Pt moiety to the Si−Si σ^*-antibonding MO. Such strong ligands as Ph^-, $[R-Ar]^-$ [R−Ar = 2,6-(2,6-iPr$_2$C$_6$H$_3$)$_2$C$_6$H$_3$], and $C(NHC)_2$ stabilize similar Y-shaped structures even without steric effect. We found that the proton affinity of the ligand is a good index to predict the Y-shaped structure. Germyl and boryl ligands can also provide the unusual Y-shaped structure, which contains somewhat stronger Ge−Ge and B−B bonding interactions in comparison with the Si−Si interaction. In the boryl complex, the vacant p orbital of the B atom also contributes to the bonding interactions between the two B atoms and between the B−B moiety and the Pt center. The Pd analogue presents the unusual Y-shaped structure, too. The Ir analogue forms a distorted trigonal-bipyramidal structure in which the equatorial moiety adopts a similar unusual Y-shaped structure with an acute Si−Ir−Si angle and a short Si···Si distance.

These complexes are best understood as σ-disilane, σ-digermane, σ-diborane, and σ-borylsilane complexes of Pt(0), Pd(0), and Ir(I). Their interesting geometries and electronic structures are good models of snapshots for the reductive eliminations of disilane, digermane, diborane, and borylsilane. Compared with $Pt[NHC(Dip)_2](SiMe_3)_2$, the digermyl, diboryl, and borylsilyl systems are understood to be moderately more productlike snapshots. Our theoretical prediction shows a lot of possibilities to synthesize such unusual Y-shaped complexes. If a series of electron-donating and/or electron-withdrawing functional groups could be incorporated into a phenyl anion ligand, for example, one could obtain a series of snapshots of the reductive elimination. Thus, all of these complexes are interesting targets for synthesis.

ASSOCIATED CONTENT

Supporting Information

Optimized geometrical parameters of the three-coordinate Pt complexes $PtLR_2$ **1**−**5** at the B3PW91/BS-I level and relative energies (ΔE_{rel}) with respect to the form **a**; calculated ^{195}Pt NMR chemical shifts (ppm) of various Pt complexes; Kohn−Sham orbitals of the unoccupied d orbital of **6b** and **7a**−**c**; optimized structures of the T-shaped Pt complexes **11**−**18**; relative energies of forms **a**−**c** with zero-point energy corrections and Gibbs energies; reliability of the calculated ^{195}Pt NMR chemical shift; π back-donation from the Pt center to the $NHC(Dip)_2$ ligand; optimized structures of the diboryl Pt complexes **26**−**28**; explanation of population analysis based on the MOs of fragments; complete refs 22 and 23; and the Cartesian coordinates and total energies of all the optimized structures in this work. This material is available free of charge via the Internet at http://pubs.acs.org.

AUTHOR INFORMATION

Corresponding Author

sakaki.shigeyoshi.47e@st.kyoto-u.ac.jp

Notes

The authors declare no competing financial interest.

ACKNOWLEDGMENTS

This work was financially supported by the Ministry of Education, Culture, Sports, Science, and Technology through a Grant-in-Aid of Specially Promoted Science and Technology (22000009). We thank the computer center of the Institute for Molecular Science (IMS, Okazaki, Japan) for kind use of computers.

REFERENCES

(1) (a) Collman, J. P.; Hegedus, L. S.; Norton, J. R.; Finke, R. G. *Principles and Applications of Organotransition Metal Chemistry*, 2nd ed.; University Science Books: Mill Valley, CA, 1987. (b) Puddephatt, R. J. *Angew. Chem.* **2002**, *114*, 271; *Angew. Chem., Int. Ed.* **2002**, *41*, 261. (c) Tagge, C. D.; Simpson, R. D.; Bergman, R. G.; Hostetler, M. J.; Girolami, G. S.; Nuzzo, R. G. *J. Am. Chem. Soc.* **1996**, *118*, 2634. (d) Maguire, J. A.; Boese, W. T.; Goldman, M. E.; Goldman, A. S. *Coord. Chem. Rev.* **1990**, *97*, 179. (e) Moncho, S.; Ujaque, G.; Lledós, A.; Espinet, P. *Chem.—Eur. J.* **2008**, *14*, 8986.

(2) For fourth coordination to three-coordinate Pt(II) complexes, see: (a) Ingleson, M. J.; Mahon, M. F.; Weller, A. S. *Chem. Commun.* **2004**, 2398. (b) Baratta, W.; Stoccoro, S.; Doppiu, A.; Herdtweck, E.; Zucca, A.; Rigo, P. *Angew. Chem.* **2003**, *115*, 109; *Angew. Chem., Int. Ed.* **2003**, *42*, 105. (c) Mole, L.; Spencer, J. L.; Carr, N.; Orpen, A. G. *Organometallics* **1991**, *10*, 49. For fourth coordination to three-coordinate Pd(II) complexes, see: (d) Stambuli, J. P.; Incarvito, C. D.; Hartwig, J. F. *J. Am. Chem. Soc.* **2004**, *126*, 1184. (e) Stambuli, J. P.; Bühl, M.; Hartwig, J. F. *J. Am. Chem. Soc.* **2002**, *124*, 9346. (f) Cámpora, J.; Gutiérrez-Puebla, E.; López, J. A.; Monge, A.; Palma, P.; Del Río, D.; Carmona, E. *Angew. Chem.* **2001**, *113*, 3753; *Angew. Chem., Int. Ed.* **2001**, *40*, 3641.

(3) (a) Fu, G. C. *Acc. Chem. Res.* **2008**, *41*, 1555. (b) Würtz, S.; Glorius, F. *Acc. Chem. Res.* **2008**, *41*, 1523. (c) Martin, R.; Buchwald, S. L. *Acc. Chem. Res.* **2008**, *41*, 1461. (d) Marion, N.; Nolan, S. P. *Acc. Chem. Res.* **2008**, *41*, 1440. (e) Kantchev, E. A. B.; O'Brien, C. J.; Organ, M. G. *Angew. Chem.* **2007**, *119*, 2824; *Angew. Chem., Int. Ed.* **2007**, *46*, 2768. (f) Littke, A. F.; Fu, G. C. *Angew. Chem.* **2002**, *114*, 4350; *Angew. Chem., Int. Ed.* **2002**, *41*, 4176.

(4) Yamashita, M.; Hartwig, J. F. *J. Am. Chem. Soc.* **2004**, *126*, 5344.

(5) Komiya, S.; Albright, T. A.; Hoffmann, R.; Kochi, J. K. *J. Am. Chem. Soc.* **1976**, *98*, 7255.

(6) Berthon-Gelloz, G.; de Bruin, B.; Tinant, B.; Markó, I. E. *Angew. Chem., Int. Ed.* **2009**, *48*, 3161.

(7) (a) Becke, A. D. *Phys. Rev. A* **1988**, *38*, 3098. (b) Becke, A. D. *J. Chem. Phys.* **1993**, *98*, 5648.

(8) Perdew, J. P.; Wang, Y. *Phys. Rev. B* **1992**, *45*, 13244.

(9) Wadt, W. R.; Hay, P. J. *J. Chem. Phys.* **1985**, *82*, 299.

(10) (a) Hehre, W. J.; Ditchfield, R.; Pople, J. A. *J. Chem. Phys.* **1972**, *56*, 2257. (b) Hariharan, P. C.; Pople, J. A. *Theor. Chim. Acta.* **1973**, *28*, 213. (c) Francl, M. M.; Petro, W. J.; Hehre, W. J.; Binkley, J. S.; Gordon, M. S.; DeFrees, D. J.; Pople, J. A. *J. Chem. Phys.* **1982**, *77*, 3654.

(11) Martin, J. M. L.; Sundemann, A. *J. Chem. Phys.* **2001**, *114*, 3408.
(12) Ehlers, A. W.; Böhme, M.; Dapprich, S.; Gobbi, A.; Höllwarth, A.; Jonas, V.; Köhler, K. F.; Stegmann, R.; Veldkamp, A.; Frenking, G. *Chem. Phys. Lett.* **1993**, *208*, 111.
(13) Andrae, D.; Haeussermann, U.; Dolg, M.; Stoll, H.; Preuss, H. J. *Theor. Chim. Acta* **1990**, *77*, 123.
(14) (a) Douglas, M.; Kroll, N. M. *Ann. Phys. (N.Y.)* **1974**, *82*, 89. (b) Hess, B. A. *Phys. Rev. A* **1985**, *32*, 756. (c) Hess, B. A. *Phys. Rev. A* **1986**, *33*, 3742. (d) Jansen, G.; Hess, B. A. *Phys. Rev. A* **1989**, *39*, 6016.
(15) (a) Tatewaki, H.; Koga, T. *Chem. Phys. Lett.* **2000**, *328*, 473. (b) Osanai, Y.; Noro, T.; Miyoshi, E.; Sekiya, M.; Koga, T. *J. Chem. Phys.* **2004**, *120*, 6408.
(16) (a) Dunning, T. H., Jr. *J. Chem. Phys.* **1989**, *90*, 1007. (b) Woon, D. E.; Dunning, T. H., Jr. *J. Chem. Phys.* **1993**, *98*, 1358.
(17) Zhao, Y.; Truhlar, D. G. *J. Chem. Phys.* **2006**, *125*, No. 194101.
(18) Lee, C.; Yang, W.; Parr, R. G. *Phys. Rev. B* **1988**, *37*, 785.
(19) Zhao, Y.; Truhlar, D. G. *Theor. Chem. Acc.* **2008**, *120*, 215.
(20) Iikura, H.; Tsuneda, T.; Yanai, T.; Hirao, K. *J. Chem. Phys.* **2001**, *115*, 3540.
(21) Boese, A. D.; Handy, N. C. *J. Chem. Phys.* **2001**, *114*, 5497.
(22) Frisch, M. J.; et al. *Gaussian 03*, revision D.02; Gaussian, Inc.: Wallingford, CT, 2003.
(23) Frisch, M. J.; et al. *Gaussian 09*, revision B.01; Gaussian, Inc.: Wallingford, CT, 2010.
(24) (a) Bond distance in the free molecule optimized using the DFT(B3PW91)/BS-I method. (b) Bond energy calculated with the BS-II basis set.
(25) (a) Chen, W.; Shimada, S.; Tanaka, M. *Science* **2002**, *295*, 308. (b) Crabtree, R. H. *Science* **2002**, *295*, 288. (c) Aullón, G.; Lledós, A.; Alvarez, S. *Angew. Chem., Int. Ed.* **2002**, *41*, 1956.
(26) Pregosin, P. S. *Coord. Chem. Rev.* **1982**, *44*, 247.
(27) Still, B. M.; Anil Kumar, P. G.; Aldrich-Wright, J. R.; Price, W. S. *Chem. Soc. Rev.* **2007**, *36*, 665.
(28) Truflandier, L. A.; Autschbach, J. *J. Am. Chem. Soc.* **2010**, *132*, 3472.
(29) Koch, K. R.; Burger, M. R.; Kramer, J.; Westra, A. N. *Dalton Trans.* **2006**, 3277.
(30) Tomasi, J.; Mennucci, B.; Cammi, R. *Chem. Rev.* **2005**, *105*, 2999.
(31) Koie, Y.; Shinode, S.; Saito, Y. *J. Chem. Soc., Dalton Trans.* **1981**, 1082.
(32) Georgii, I.; Mann, B. E.; Taylor, B. F. *Inorg. Chim. Acta* **1984**, *86*, L81.
(33) Klein, A.; Schurr, T.; Knödler, A.; Gudat, D.; Klinkhammer, K.; Jain, V. K.; Záliš, S.; Kaim, W. *Organometallics* **2005**, *24*, 4125.
(34) Salvadori, P.; Uccello-Barretta, G.; Bertozzi, S.; Settambolo, R.; Lazzaroni, R. *J. Org. Chem.* **1988**, *53*, 5768.
(35) For reviews of bulky terphenyl ligands, see: (a) Power, P. P. *Chem. Rev.* **2012**, *112*, 3482. (b) Power, P. P. *Chem. Rev.* **2003**, *103*, 739. (c) Power, P. P. *Chem. Rev.* **1999**, *99*, 3463. (d) Power, P. P. *Nature* **2010**, *463*, 171.
(36) Tonner, R.; Frenking, G. *Angew. Chem., Int. Ed.* **2007**, *46*, 8695.
(37) The NBO charge of the R ligand in Pt[NHC(Dip)$_2$]R$_2$ decreases in the order CMe_3 (−0.40, −0.08) > $BO_2C_2H_2$ (−0.06) > $GeMe_3$ (+0.01) > $SiMe_3$ (+0.02), indicating that the donation becomes stronger in the same order.